6396 *J. Am. Chem. Soc.* **1996,** *118,* 6396−6406

Generation of Oxozirconocene Complexes from the Reaction of $Cp_2(THF)Zr{=}N$-*t*-Bu with Organic and Metal Carbonyl Functionalities: Apparently Divergent Behavior of Transient $[Cp_2Zr{=}O]$

Sun Yeoul Lee and Robert G. Bergman*

Contribution from the Department of Chemistry, University of California, Berkeley, California 94720

Received December 4, 1995[⊗]

Abstract: The reactivity of $Cp_2(THF)Zr{=}N$-*t*-Bu (**1a**) toward a series of organic and metal carbonyl complexes has been examined. The Zr═N linkage of **1a** undergoes imido/oxo exchange reactions with the carbonyl compounds and generates three different types of oxozirconocene products: $(Cp_2Zr{=}O)_n$ (**3**), $(Cp_2Zr)_2(\mu\text{-}O)(\mu\text{-}N\text{-}t\text{-}Bu)$ (**9**), and $(Cp_2Zr)_2O_3CCPh_2$ (**12**) were obtained from the reactions of **1a** with $RR'C{=}O$ ($R = R' = Me$ (**2b**); $R = Ph$, $R' = H$ (**2c**); $R = i\text{-}Pr$, $R' = H$ (**2d**)), $CpCo(CO)_2$ (**7**), and $Ph_2C{=}C{=}O$ (**10**), respectively. The coproducts in these reactions were imines $RR'C{=}N$-*t*-Bu (**4b−d**), isonitrile complexes $CpCo(CO)(CN$-*t*-Bu) (**8a**), and ketenimines $Ph_2C{=}C{=}N$-*t*-Bu (**11a**), respectively. With more highly hindered carbonyls containing α-hydrogen atoms, the reaction followed a different pathway leading to the formation of the enolate complexes $Cp_2Zr(NH\text{-}t\text{-}Bu)(OCR_3CR_2R_1)$ ($R_1 = H$, R_2 and $R_3 = (CH_2)_3CH(CCH_3)_3$ (**5e**); $R_1 = R_2 = H$, $R_3 = C(CH_3)_3$ (**5f**); $R_1 = R_2 = CH_3$, $R_3 = CH(CH_3)_2$ (**5g**)). Possible mechanisms for these transformations, as well as the factors that might control the dependence of the fate of "$Cp_2Zr{=}O$" on its method of generation, are discussed.

Introduction

The chemistry of complexes containing metal−nitrogen multiply-bonded groups ($M{=}NR_2$) has developed dramatically in recent years.[1] These compounds are useful for imido group transfer in catalytic processes[2−5] as well as in organic synthesis.[6−8] Furthermore, the exchange of multiply-bonded ligands between metals offers a potentially useful synthetic approach to new transition metal compounds.[9]

An earlier publication from our group briefly reported that the monomeric imido complex $Cp_2(THF)Zr{=}N$-*t*-Bu (**1a**) undergoes a spontaneous imido/oxo exchange reaction with $Ph_2C{=}O$ (**2a**) and *t*-$BuN{=}C{=}O$ to generate the oxozirconocene oligomer $(Cp_2Zr{=}O)_n$ (**3**) and the corresponding imine (**4a**) and carbodiimide products, respectively.[10,11] As shown in eq 1, it was assumed that $[Cp_2Zr{=}O]$ is generated during the reaction and rapidly oligomerizes to form **3**. Monomeric group 4 oxometallocenes are notorious for their self-oligomerization and have eluded successful trapping except for a few examples containing the sterically bulky (η^5-C_5Me_5) ligand (e.g. $[Cp^*_2M{=}O]$ (M = Zr, V)).[12−16] In this paper we report additional studies that indicate that the behavior of the transient "$Cp_2Zr{=}O$" species generated during these reactions depends on the character of the oxygen source.

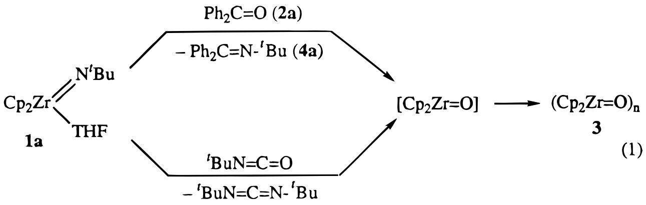

(1)

Results

Reactions with Organic Carbonyl Compounds. The carbonyl compounds (ketones and aldehydes) shown in Scheme 1 are divided into three groups (A, B, and C) based on their steric encumbrance. Group A includes aldehydes and simple ketones (**2b−d**). In group B are illustrated moderately sterically hindered ketones containing either one bulky group (**2e** and **2f**) or two secondary alkyl groups (**2g**). Ketones in groups A and B possess α-protons. The type C compound illustrated is a sterically encumbered ketone without α-hydrogens (**2h**).

As with **2a**, the reaction of the carbonyl compounds in group A (**2b−d**) with **1a** generates the corresponding imine products (**4b−d**) and **3** as shown eq 2. These reactions occur spontaneously at room temperature and quantitative amounts (>90% by ^{1}H NMR) of the corresponding imine products were cleanly produced. However, the $(Cp_2Zr{=}O)_n$ (**3**) produced is generated as several different oligomers (based on several Cp resonances around 6 ppm) that fall out of solution as a white precipitate. Among those Cp resonances, the peak at 6.31 ppm in THF-d_8 (or 6.27 ppm in C_6D_6) was always observed as a major

---

[⊗] Abstract published in *Advance ACS Abstracts,* June 1, 1996.

(1) For an excellent and comprehensive recent review, see: Wigley, D. E. In *Progress in Inorganic Chemistry*; Karlin, K. D., Ed.; Wiley: New York, 1994; Vol. 42.

(2) Ivin, K. J. *Olefin Metathesis*; Academic Press: London, 1983.

(3) Ge, Y.-W.; Sharp, P. R. *Inorg. Chem.* **1992**, *31*, 379.

(4) Breslow, R.; Gellman, S. H. *J. Am. Chem. Soc.* **1983**, *105*, 6728.

(5) Svatits, E. W.; Dawson, J. H.; Breslow, R.; Gellman, S. H. *J. Am. Chem. Soc.* **1985**, *107*, 6427.

(6) Evans, D. A.; Faul, M. M.; Bilodeau, M. T. *J. Org. Chem.* **1991**, *56*, 6744.

(7) Mcgrane, P. L.; Livinghouse, T. *J. Org. Chem.* **1992**, *57*, 1323.

(8) Mcgrane, P. L.; Jensen, M.; Livinghouse, T. *J. Am. Chem. Soc.* **1992**, *114*, 5459.

(9) Jolly, M.; Mitchell, J. P.; Gibson, V. C. *J. Chem. Soc., Dalton Trans.* **1992**, 1331.

(10) Walsh, P. J.; Hollander, F. J.; Bergman, R. G. *Organometallics* **1993**, *12*, 3705.

(11) Walsh, P. J. Thesis, University of California, Berkeley, 1990.

(12) Carney, M. J.; Walsh, P. J.; Hollander, F. J.; Bergman, R. G. *J. Am. Chem. Soc.* **1989**, *111*, 8751.

(13) Carney, M. J.; Walsh, P. J.; Hollander, F. J.; Bergman, R. G. *Organometallics* **1992**, *11*, 761.

(14) Smith, M. R., III; Matsunaga, P. T.; Andersen, R. A. *J. Am. Chem. Soc.* **1993**, *115*, 7049.

(15) Howard, W. A.; Parkin, G. *J. Am. Chem. Soc.* **1994**, *116*, 606.

(16) Polse, J. L.; Andersen, R. A.; Bergman, R. G. *J. Am. Chem. Soc.* **1995**, *117*, 5393.

S0002-7863(95)04050-9 CCC: $12.00

Scheme 1

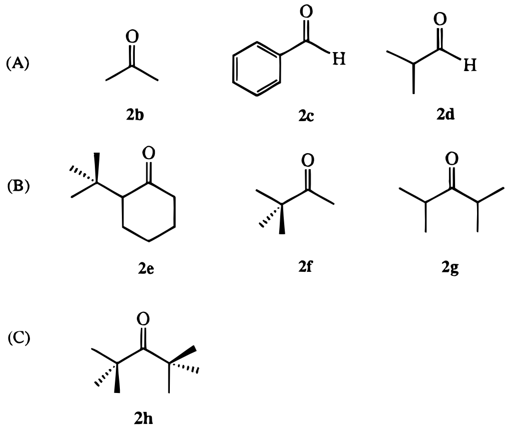

component. This matches the chemical shift of the known cyclotrimeric compound $(Cp_2Zr{=}O)_3$.[17-20] No further attempt to characterize **3** was made, but the imine products were identified by GCMS and by comparison with literature spectral data.[21,22] The identity of one of the imine products (PhCH=N-*t*-Bu (**4c**)) was also confirmed by independent preparation.[23]

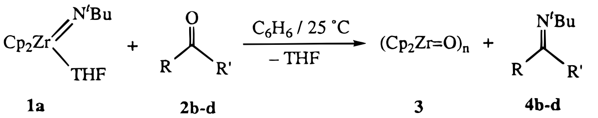

(2)

(b) R = Me, R' = Me
(c) R = Ph, R' = H
(d) R = *i*-Pr, R' = H

The reactions of **1a** with compounds **2e**−**g** in the group B also occur cleanly at 25 °C in >95% yield (by ^{1}H NMR), but do not generate the imine products or **3**. Instead, the zirconocene enolate complexes **5e**−**g** are formed by α-hydrogen abstraction (eq 3). The enolate complexes were isolated in analytically pure form by recrystallization from pentane (or TMS_2O) at −35 °C in 60−75% isolated yields. The ^{1}H NMR spectra of these enolates generally contain resonances near 6 ppm (10H) attributable to the cyclopentadienyl groups, a broad singlet in the region 4−5 ppm (1H) due to the alkylamido hydrogen, and a singlet near 1.2 ppm due to the *tert*-butylamido group. In addition to these resonances, enolates **5e** and **5f** (when R_1 or R_2 = H) exhibit new vinyl protons at 4.52 ppm (for **5e**) and 3.78 and 3.47 ppm (for **5f**; C_6D_6). The $^{13}C\{^1H\}$ NMR spectra of **5e**−**g** show a resonance near 160−180 ppm due to the α−carbon and a resonance in the 80−110 ppm region attributable to the *β*-vinyl carbon.

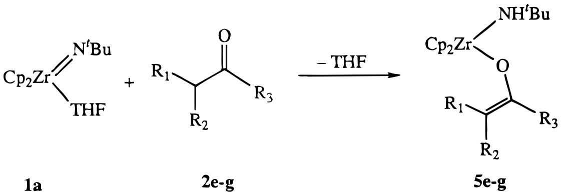

(3)

(e) R_1 = H, R_2 and R_3 = $(CH_2)_3CH(CCH_3)_3$
(f) $R_1 = R_2$ = H, $R_3 = C(CH_3)_3$
(g) $R_1 = R_2 = CH_3$, $R_3 = CH(CH_3)_2$

In contrast to the carbonyl compounds in groups A and B, which react easily with imido complex **1a** at the ambient temperature, 2,2,4,4-tetramethyl-3-pentanone (**2h**) is inert to **1a** up to 75 °C for 1.5 days, presumably due to the steric inaccessibility of the carbonyl moiety. Harsher conditions led to decomposition of the starting material.

Crystal and Molecular Structure of 5e. Transition metal enolates have been shown to bind to metal centers in an η^1-mode through the oxygen atom[15,24-29] or methylene group,[30] or in an η^3-(oxo-π-allyl) mode.[31-33] Typically, early transition metal enolates exist in the O-bound form while late metal enolates are C-bound (a few cases of late transition metal O-bound enolates are known).[34-38] To confirm the structure of our enolate complexes, clear crystals of **5e** were grown in pentane at −35 °C and an X-ray crystallographic analysis was performed. The data collection parameters are reported in Table 1. Solution of the structure revealed complete disorder of the enolate ligand about a pseudo-mirror plane containing the O- and C16-atoms as shown in Figure 1. The disorder was best modeled as having 82:18 occupancy of two conformations, the major one containing C11−C20 and the minor one containing C211−C220 (see the supporting information). The major conformation also showed another type of disorder in the enolate ring. This second disorder was fit to a 50:50 occupancy of C14 in two sites. The ORTEP diagram of one of the major conformations of **5e** is shown in Figure 2. Although bond distances and angles shown Tables 2 and 3 are less reliable than they might otherwise be due to the disorder, it is clear that the enolate fragment is bound to zirconium through oxygen (Zr−O: 1.998(3) Å)[15,24-26] in an η^1-mode and the double bond is localized between C11 and C12 (1.334(7) Å). The Zr−N−C21 bond angle of 142.5(3)° in **5e** is bent more strongly than that in the analogous amido complexes, $Cp_2Zr(C_6H_3Cl_2)$(NH-*t*-Bu) (147.6(2)°)[39] and $Cp_2Zr(1\text{-}C_9H_7)$(NH-*t*-Bu) (*ca.* 147.7°).[39,40]

---

[17] Fachinetti, G.; Floriani, C.; Chiesi-Villa, A.; Guastini, C. *J. Am. Chem. Soc.* **1979**, *101*, 1767.

[18] Kropp, K.; Skibbe, V.; Erker, G.; Krüger, C. *J. Am. Chem. Soc.* **1983**, *105*, 3353.

[19] Erker, G.; Dorf, U.; Atwood, J. L.; Hunter, W. E. *J. Am. Chem. Soc.* **1986**, *108*, 2251.

[20] Boutonnet, F.; Zablocka, M.; Igau, A.; Jaud, J.; Majoral, J.-P.; Schamberger, J.; Erker, G.; Werner, S.; Krüger, C. *J. Chem. Soc., Chem. Commun.* **1995**, 823.

[21] Klusener, P. A. A.; Tip, L.; Brandsma, L. *Tetrahedron* **1991**, *47*, 2041.

[22] Larsen, J.; Jorgensen, K. A. *J. Chem. Soc., Perkin Trans. 2* **1992**, 1213.

[23] A referee has pointed out the similarity of this transformation to the aza-Wittig reaction. For a recent example of the aza-Wittig reaction and leading references, see: Sakai, T.; Kodama, T.; Fujimoto, T.; Ohta, K.; Yamamoto, I. *J. Org. Chem.* **1994**, *59*, 7144.

[24] Veya, P.; Floriani, C.; Chiesi-Villa, A.; Guastini, C. *Organometallics* **1991**, *10*, 2991.

[25] Curtis, M. D.; Thanedar, S.; Butler, W. M. *Organometallics* **1984**, *3*, 1855.

[26] Manriquez, J. M.; McAlister, D. R.; Sanner, R. D.; Bercaw, J. E. *J. Am. Soc. Chem.* **1978**, *100*, 2716.

[27] Sonnenberger, D. C.; Mintz, E. A.; Marks, T. J. *J. Am. Chem. Soc.* **1984**, *106*, 3484.

[28] Stille, J. R.; Grubbs, R. H. *J. Am. Chem. Soc.* **1983**, *105*, 1664.

[29] de With, J.; Horton, A. D. *Angew. Chem., Int. Ed. Engl.* **1993**, *32*, 903.

[30] Burkhardt, E. R.; Doney, J. J.; Bergman, R. G.; Heathcock, C. H. *J. Am. Chem. Soc.* **1987**, *109*, 2022 and references therein.

[31] Ito, Y.; Aoyama, H.; Hirao, T.; Mochizuki, A.; Saegusa, T. *J. Am. Chem. Soc.* **1979**, *101*, 494.

[32] Guggolz, E.; Ziegler, M. L. *J. Organomet. Chem.* **1980**, *194*, 317.

[33] Robertson, G. B.; Whimp, P. O. *Inorg. Chem.* **1973**, *12*, 1740.

[34] Slough, G. A.; Bergman, R. G.; Heathcock, C. H. *J. Am. Chem. Soc.* **1989**, *111*, 938.

[35] Hartwig, J. F.; Andersen, R. A.; Bergman, R. G. *J. Am. Chem. Soc.* **1990**, *112*, 5670.

[36] Hartwig, J. F.; Bergman, R. G.; Andersen, R. A. *J. Am. Chem. Soc.* **1990**, *112*, 3234.

[37] Dall'antonia, P.; Graziani, M. *J. Organomet. Chem.* **1980**, *186*, 131.

[38] Ito, Y.; Nakatsuka, M.; Kise, N.; Saegusa, T. *Tetrahedron Lett.* **1980**, *21*, 2873.

[39] Lee, S. Y.; Bergman, R. G. *J. Am. Chem. Soc.* **1995**, *117*, 5877.

[40] Lee, S. Y.; Bergman, R. G. Mauscript in preparation.

Table 1. Crystal and Data Parameters for Complexes **5e** and **12**

compd nos.	**5e**	**12**
empirical formula	$C_{24}H_{36}NOZr$	$C_{72}H_{68}O_7Zr_4{}^{a}$
formula wt (amu)	445.77	1410.2
crystal dimens (mm)	0.20 × 0.25 × 0.30	0.12 × 0.20 × 0.38
a (Å)	9.4933(2)	16.621(4)
b (Å)	8.0068(2)	18.763(3)
c (Å)	30.6878(9)	19.417(5)
α (deg)	90	90
β (deg)	91.643(1)	90
γ (deg)	90	90
V (Å^3)	2331.65(9)	6055.7(39)
space group	$P2_1/n$	$Pbca$
Z	4	4
diffractometer	Siemens SMART	CAD4
detector	CCD area detector	crystal scintillation counter, with PHA
temp (°C)	−130	−130
scan type	ω	$\theta-2\theta$
scan width (deg)	0.3	$0.90 + 0.35 \tan \theta$
2θ range	3−46.5	3−45
no. of unique reflcns	3600	2578
T_{min}/T_{max}	0.931	0.936
no. of variables	270	179
R; R_w	0.041; 0.058	0.059; 0.069
R_{all}	$R_{int} = 0.034$	0.092
goodness of fit	2.46	2.24

[a] Represents two dimers and one THF molecule of solvation.

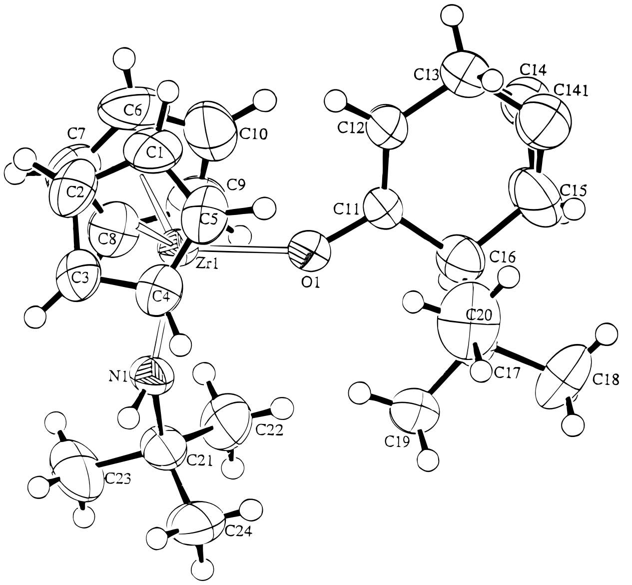

Figure 1. ORTEP view of the molecular structure of **5e** showing one of the major conformations in the disordered crystal. The ellipsoids are scaled to represent the 50% probability surface.

Furthermore, the amido ligand is twisted significantly from the O−Zr−N plane. This appears to be due to steric crowding by the enolate ligand in **5e**.

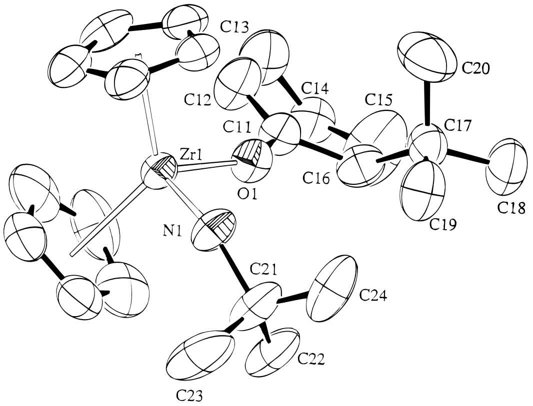

Figure 2. ORTEP view of one conformation of **5e**. The ellipsoids are scaled to represent the 50% probability surface.

Table 2. Selected Bond Distances (Å) for **5e**

Major Conformation		Minor Conformation	
Zr1−O1	1.998(3)		
Zr1−Nl	2.060(3)		
Zr1−Cp1	2.2534(4)		
Zr1−Cp2	2.3562(4)		
Nl−C21	1.499(5)		
O1−C11	1.321(5)	O1−C211	1.36(3)
C11−C12	1.334(7)	C211−C212	1.30(4)
C11−C16	1.524(6)	C211−C16	1.46(3)
C12−C13	1.495(8)	C212−C213	1.73(4)
C13−C14	1.48(1)	C213−C214	1.86(4)
C14−C15	1.48(2)	C214−C215	1.27(4)
C15−C16	1.523(8)	C215−C16	1.69(4)
C16−C17	1.542(7)	C16−C217	1.63(3)
C17−C18	1.497(8)	C217−C218	1.53(4)
C17−C19	1.500(9)	C217−C219	1.68(5)
C17−C20	1.543(9)	C217−C220	1.49(4)
C13−C141	1.46(2)		
C141−C15	1.37(2)		

Table 3. Selected Bond Angles (deg) for **5e**

Major Conformation		Minor Conformation	
O1−Zr1−N1	99.9(1)		
O1−Zr1−C10	80.4(2)		
O1−Zr1−Cp1	107.56(8)		
O1−Zr1−Cp2	106.05(8)		
N1−Zr1−Cp1	102.73(10)		
N1−Zr1−Cp2	108.3(l)		
Cp1−Zr1−Cp2	128.76(2)		
Zr1−N1−C21	142.5(3)		
Zr1−O1−C11	148.0(3)	Zr1−O1−C211	150(1)
O1−C11−C12	122.7(5)	O1−C211−C212	116(2)
O1−C11−C16	114.7(4)	O1−C211−C16	116(2)
C12−C11−C16	122.6(5)	C212−C211−C16	126(2)
C11−C12−C13	124.2(5)	C211−C212−C213	123(2)
C12−C13−C14	110.6(7)	C212−C213−C214	103(1)
C13−C14−C15	110.2(9)	C213−C214−C215	101(2)
C14−C15−C16	123.1(8)		
C11−C16−C17	115.0(4)	C211−C16−C217	112(1)
C15−C16−C17	117.0(5)	C215−C16−C217	112(1)
C16−C17−C19	113.0(5)	C16−C217−C219	108(2)
C16−C17−C20	110.4(5)	C16−C217−C220	107(2)
C18−C17−C19	106.1(6)	C218−C217−C219	98(2)
C18−C17−C20	109.4(6)	C218−C217−C220	139(2)
C19−C17−C20	107.1(5)	C219−C217−C220	84(2)
Zr1−N1−H11	132.8		
C21−N1−H11	84.5		
C12−C13−C141	114.5(8)		
C13−C141−C15	118(1)		

Low-Temperature ^{1}H NMR Study of the Reaction of 1a with 2b and 2d. The reaction of **1a** with the carbonyl compounds in group A occurs very rapidly even in THF-d_8 where excess THF significantly inhibits the dissociation of THF from the imido complex. However, the color of the reaction mixture temporarily changes from yellow to red-orange upon the addition of the ketone. The reaction was therefore monitored at 220−263 K by ^{1}H NMR spectrometry in THF-d_8. This revealed that an intermediate is first generated and then slowly converted (above 243 K) to the corresponding imine **4b** (or **4d**) and **3**. From the reaction of **1a** with **2b**, the new intermediate (**6b**) gives rise to resonances at δ 6.28 (s, 10H, C_5H_5), 1.34 (s, 6H, $(CH_3)_2$), and 1.22 (s, 9H, $C(CH_3)_3$). The intermediate (**6d**) generated from the reaction of **2d** shows resonances at δ 6.96 (d, J = 9.28 Hz, 1H, CH), 6.30 (br s, 10H, C_5H_5; Cp's accidentally degenerate), 2.88 (m, 1H, CH($CH_3)_2$), 1.22 (s, 9H, $C(CH_3)_3$), and 0.96 (d, J = 9.30 Hz, 6H, $CH(CH_3)_2$). From these data, the intermediates are tentatively assigned as the metallacycles formed by formal [2 + 2] cycloaddition of $Cp_2Zr{=}N\text{-}t\text{-}Bu$ with **2b** (or **2d**) as shown below. However, it was unclear at this stage whether they exist in monomeric or dimeric

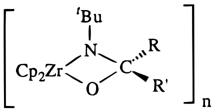

6b: R = R' = CH_3
6d: R = H, R' = $CH(CH_3)_2$
n = 1 or 2

form (*vide infra*). A second intermediate was also observed in the reaction of **1a** with **2d**, but an assignment of its structure was not possible due to the complex nature of the spectrum. There was no indication that either an enolate complex or the dimer complex $(Cp_2Zr)_2(\mu\text{-O})(\mu\text{-N-}t\text{-Bu})$ are generated during either reaction. In contrast to the observation of metallacycle intermediates (**6b** and **6d**) in the reaction of **1a** with **2b** and **2d**, no intermediate was observed in the reaction of **1a** with benzophenone (**2a**) even at 238 K where the reaction proceeds relatively slowly ($t_{1/2}$ = *ca.* 30 min).

Reactions with Metal Complexes Containing CO Groups. A study of the reactivity of **1a** toward CO functionalities in metal complexes was also carried out. We reported earlier that treatment of **1a** with $CpMn(CO)_3$ or $CpRe(CO)_3$ at 75 °C in cyclohexane results in the selective activation of the cyclopentadienyl C−H bonds of these molecules.[39] However, when **1a** is treated with $CpCo(CO)_2$ (**7**) in cyclohexane, the reaction instantly gives a complex mixture of products and a precipitate falls out of solution. The ^1H NMR spectrum of this precipitate in C_6D_6 showed several Cp resonances indicating that the material is a mixture.

When **1a** is treated with excess (*ca.* 3 equiv) $CpCo(CO)_2$ (**7**) in THF at 75 °C, the reaction mixture remains homogeneous. In this solvent the process appears to be considerably cleaner, and CpCo(CO)(CN-*t*-Bu) (**8a**)[41,42] and a new binuclear complex identified as $(Cp_2Zr)_2(\mu\text{-O})(\mu\text{-N-}t\text{-Bu})$ (**9**) are formed in 90% yield (by ^1H NMR) (eq 4). Compounds **8a** and **9** were separated based on their solubility in pentane. The pentane-soluble isonitrile compound **8a** was isolated in 28% yield and identified by comparison of its spectra with data in the literature.[41] Pentane-insoluble **9** was crystallized from pentane/benzene in 30% isolated yield. Dimer **9** shows a simple ^1H NMR spectrum (C_6D_6) with two singlets at 6.10 and 1.12 ppm attributable to the cyclopentadienyl (20H) and *tert*-butyl (9H) protons, respectively. To confirm the structure of **9**, crystals for an X-ray study were grown by slow evaporation of solvent from an ether solution of the complex. Unfortunately, an X-ray crystallographic analysis of **9** could not be fully refined due to disorder. However, it allowed us to confirm the basic structure of the metallacycle.

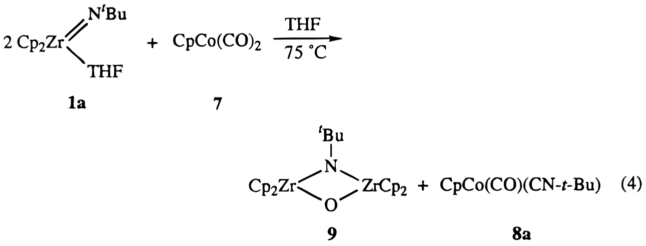

Attempts to confirm the source of the oxygen in **9** were also made. To make sure that the oxygen did not come from the reaction solvent THF, the reaction was carried out with an analogue of **1a**, $Cp_2Zr(N\text{-}2,6\text{-}(CH_3)_2C_6H_3)(THF)$ (**1b**). The fact that this arylimido complex does not react with benzene C−H bonds allowed us to carry out the reaction of **1b** with $CpCo(CO)_2$ (**7**) in an aromatic rather than an oxygen-containing solvent. The reaction of **1b** with cobalt complex **7** at 75 °C in C_6H_6 (as well as THF-d_8) leads to the formation of $CpCo(CO)(CN\text{-}2,6\text{-}(CH_3)_2C_6H_3)$[43] (**8b**) (46% isolated) and "$Cp_2Zr{=}O$ oligomer" **3** (eq 5). Although **3** was observed instead of the analogue of dimer **9** in both solvents, the experiment in C_6H_6 clearly demonstrates that THF is not required for the conversion of the starting terminal imido complex into an oxozirconium product. The imido complex **1a** also reacts with 86% ^{13}CO labeled $CpCo(^{13}CO)_2$ under the same conditions to give **9** and $CpCo(^{13}CO)(^{13}CN\text{-}t\text{-}Bu)$ (**8a-^{13}C**) with 84% incorporation of label, as determined by integration of relative mass peaks from EI mass spectroscopy.

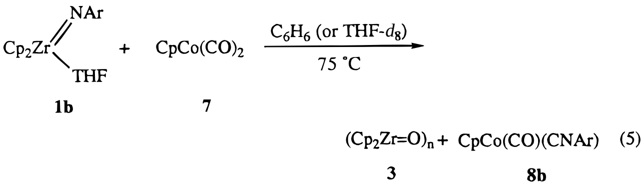

Ar = 2,6-$(CH_3)_2C_6H_3$

Preliminary ^1H NMR investigations suggest that the reaction of **1a** with $CpV(CO)_4$, $CpFe(CH_3)(CO)_2$, and $(C_6H_6)Cr(CO)_3$ in THF-d_8 also yields **9** and the corresponding deoxygenated metal carbonyl isocyanide complexes $CpV(CO)_3$(CN-*t*-Bu),[44] $CpFe(CH_3)(CO)$(CN-*t*-Bu),[45] or $(C_6H_6)Cr(CO)_2$(CN-*t*-Bu),[46] respectively. The rates of the reaction of **1a** with $CpV(CO)_4$ and $(C_6H_6)Cr(CO)_3$ are relatively fast, and the reactions occur even at 25 °C over several hours. The reaction of **1a** with the simple metal carbonyl complex $Mo(CO)_6$ in THF-d_8 at 25 °C was also examined briefly by ^1H NMR spectroscopy. In this case, more than one *tert*-butyl resonance grows in during the reaction, presumably due to the formation of a mixture of isocyanide complexes $Mo(CO)_{5-n}(CN\text{-}t\text{-}Bu)_n$. Dimer **9** was also formed cleanly as expected.

The observation of oxygen abstraction from metal complexes containing carbonyl groups in THF induced us to re-examine the reactions of $CpM(CO)_3$ (M = Mn, Re) with **1a** in this solvent rather than cyclohexane. The reaction of **1a** with $CpM(CO)_3$ (M = Mn, Re) in THF requires more vigorous reaction conditions (105 °C, 4 days) than the same reaction in C_6H_{12} (75 °C, 1.5 days) since the coordinating ability of THF inhibits the formation of free $Cp_2Zr{=}N\text{-}t\text{-}Bu$, significantly decreasing the reaction rate. The reaction in THF still generates the cyclopentadienyl C−H activated products[39,40] as the major species, but somewhat less than 30% of ligand exchange product **9** was also obtained (eq 6). New ^1H NMR resonances for *tert*-butyl groups were also observed near 1.15 ppm, presumably due to the formation of the corresponding isonitrile complexes

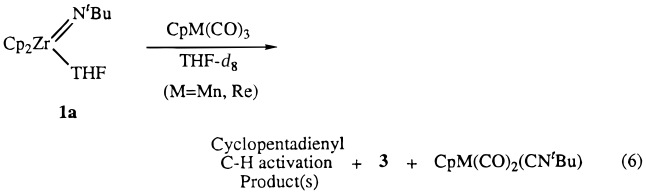

Cyclopentadienyl C-H activation Product(s):
$Cp_2Zr(NH\text{-}t\text{-}Bu)(\eta^1{:}\eta^5\text{-}C_5H_4M(CO)_2)$ (M = Mn, Re)
$(Cp_2Zr)_2(NH\text{-}t\text{-}Bu)_2(\eta^1{:}\eta^1{:}\eta^5\text{-}C_5H_3M(CO)_2)$ (M = Re)

---

(41) Beaumont, I.; Wright, A. H. *J. Organomet. Chem.* **1992**, *425*, C11.

(42) Doherty, J.; Fortune, J.; R., M. A.; Stephens, F. S. *J. Chem. Soc., Dalton Trans.* **1984**, 1111.

$CpM(CO)_2(CN\text{-}t\text{-}Bu)$ (M = Mn,[47,48] Re[48]). However, they were not clearly identified due to the complex nature of the spectra.

Reaction of 1a with Diphenylketene (10). The reactivity of **1a** toward a C=C=O functionality was also studied. When the imido complex **1a** is mixed with an excess of $Ph_2C{=}C{=}O$ (**10**)[49] in benzene, it spontaneously reacts with $^3/_2$ equiv of **10** to form $Ph_2C{=}C{=}N\text{-}t\text{-}Bu$ (**11a**) and $^1/_2$ equiv of $(Cp_2Zr)_2O_3\text{-}CCPh_2$ (**12**) (eq 7). In this case no $[Cp_2Zr{=}O]_n$ (**3**) was observed. The ketenimine product **11a** was isolated as a pale yellow liquid in 70% yield. The existence of the C=C=N bond in **11a** is indicated by the NMR resonance of a quaternary carbon at 182.7 ppm in the $^{13}C\{^1H\}$ NMR spectrum (C_6D_{12}) and the C=N stretching at 2014 cm^{-1} in the IR spectrum (THF).

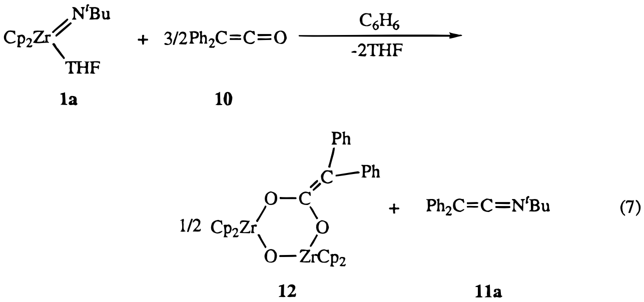

Tris-oxo complex **12** was also isolated as the hemisolvate [**12**·0.5 THF] in analytically pure form by recrystallization from THF/pentane at −35 °C in 65% isolated yield. Its ^1H and $^{13}C\{^1H\}$NMR spectra establish that **12** contains cyclopentadienyl and phenyl groups in a 2:1 ratio. The infrared spectrum of **12** shows no ketene C=O stretch in the expected 2100 cm^{-1} region. Mass spectrometry (EI) shows an ion with *m/e* 665.7 which is consistent with the formula shown in eq 7. The structure of **12** was confirmed by X-ray crystallography. The data collection parameters are reported in Table 1. As shown in Figure 3, the ORTEP diagram of [**12**·0.5 THF] clearly demonstrates that the compound contains a 6-membered ring composed of two molecules of $[Cp_2Zr{=}O]$ and one molecule of $Ph_2C{=}C{=}O$ (**10**). The C−O (*ca.* 1.36 Å) and Zr−O (*ca.* 2.00 Å) bond lengths are consistent with single bonds, but C21=C22 (1.365(7) Å) shows double bond character. The 6-membered ring is slightly twisted with *ca.* 50° (O−Zr−O−C21) and *ca.* 15° (O−Zr−O−Zr) torsion angles. Relevant bond lengths and bond angles are listed in Table 4. Selected torsion angles are listed in Table 5.

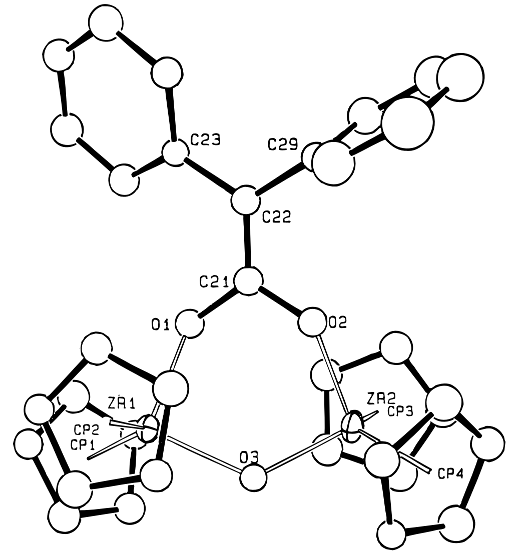

Figure 3. ORTEP view of the molecular structure of **12**. The ellipsoids are scaled to represent the 50% probability surface.

Table 4. Selected Intramolecular Distances (Å) and Angles (deg) for Complex **12**

Bond Distances (Å)			
Zr1−Zr2	3.536(2)	Zr1−O1	2.042(8)
Zr1−O3	1.983(8)	Zr2−O2	2.037(9)
Zr2−O3	1.958(7)	Zr1−Cpl	2.245
Zr1−Cp2	2.231	Zr2−Cp3	2.232
Zr2−Cp4	2.257	C21−O1	1.362(15)
C21−O2	1.358(14)	C21−C22	1.365(17)
C22−C23	1.502(17)	C22−C29	1.506(17)
Bond Angles (deg)			
Cpl−Zr1−O1	103.8	Cp2−Zr1−O1	105.7
Cp1−Zr1−O3	109.3	Cp2−Zr1−O3	108.8
Cp1−Zr1−Cp2	129.47	O1−Zr1−O3	93.5(3)
Cp3−Zr2−O2	106.6	Cp4−Zr2−O2	104.9
Cp3−Zr2−O3	108.3	Cp4−Zr2−O3	108.9
Cp3−Zr2−Cp4	128.56	O2−Zr2−O3	94.0(3)
Zr1−O3−Zr2	127.6(4)	Zr1−O1−C21	128.2(8)
Zr2−O2−C21	133.8(9)	O1−C21−O2	114.5(12)
O1−C21−C22	125.4(11)	O2−C21−C22	120.1(12)
C21−C22−C23	122.5(12)	C21−C22−C29	118.5(12)
C23−C22−C29	119.0(12)		

Table 5. Selected Torsion Angles for Complex **12** in Degrees

atom 1	atom 2	atom 3	atom 4	angle
O3	Zrl	O1	C21	−55.84(1.07)
O1	Zrl	O3	Zr2	15.73(0.59)
O3	Zr2	O2	C21	−44.38(1.02)
O2	Zr2	O3	Zrl	13.96(0.57)
Zrl	O1	C21	O2	42.54(1.56)
Zrl	O1	C21	C22	−136.69(1.13)
Zr2	O2	C21	O1	20.21(1.62)
Zr2	O2	C21	C22	−160.52(0.95)

The formation of ketenimine **11a** and the tris-oxo complex **12** was not affected by variation of the initial ratio of the ketene **10** to the imido complex **1a**. Even in the reaction of **1a** with 0.5 equiv of **10**, products **11a** and **12** are still generated and *ca.* $^2/_3$ of unreacted **1a** remains after the completion of the reaction. Changing the solvent to THF retards the reaction (2 days at 25 °C for completion), but the same products are generated without observation of any intermediate. The reaction of **1a** with **10** in toluene-d_8 between −30 and −10 °C proceeds at a reasonable rate ($t_{1/2}$ = *ca.* 30 min at −10 °C) allowing us to monitor the reaction by ^1H NMR spectroscopy. However, no intermediate is observed at low temperature. Furthermore, product **12** is thermally very stable. There is no evidence of further reaction, and decomposition to generate $[Cp_2Zr{=}O]_n$ (**3**) is not observed until **12** has been held at 105 °C for 4 days.

Reaction of 1a with $Ph_2C{=}C{=}NTol$ (11b). To obtain information on a transformation that might be analogous to the reaction of **1a** with diphenylketene (and also which might be more amenable to mechanistic scrutiny) we decided to explore the reactivity of **1a** toward a ketenimine. Since $Ph_2C{=}C{=}N\text{-}t\text{-}Bu$ (**11a**), generated as a byproduct during the reaction of **1a** with **10**, is inert toward **1a** at ambient temperature due to its steric hindrance, the less hindered ketenimine $Ph_2C{=}C{=}NTol$

---

(43) Yamamoto, Y.; Mise, T.; Yamamzaki, H. *Bull. Chem. Soc. Jpn.* **1978**, *51*, 2743.

(44) Coville, N. J.; Harris, G. W. *J. Organomet. Chem.* **1985**, *293*, 365.

(45) Yamamoto, Y.; Yamazaki, H. *J. Organomet. Chem.* **1975**, *90*, 329.

(46) Harris, G. W.; Albers, M. O.; Boeyens, J. C. A.; Coville, N. J. *Organometallics* **1983**, *2*, 609.

(47) Harris, G. W.; Boeyens, J. C. A.; Coville, N. J. *J. Organomet. Chem.* **1983**, *255*, 87.

(48) Terry, M. R.; Mercando, L. A.; Kelley, C.; Geoffroy, G. L.; Nombel, P.; Lugan, N.; Mathieu, R.; Ostrander, R. L.; Owens-Waltermire, B. E.; Rheingold, A. L. *Organometallics* **1994**, *13*, 843.

(49) Taylor, E. C.; Mckillop, A.; Hawks, G. H. *Org. Synth.* **1972**, *52*, 36.

Scheme 2

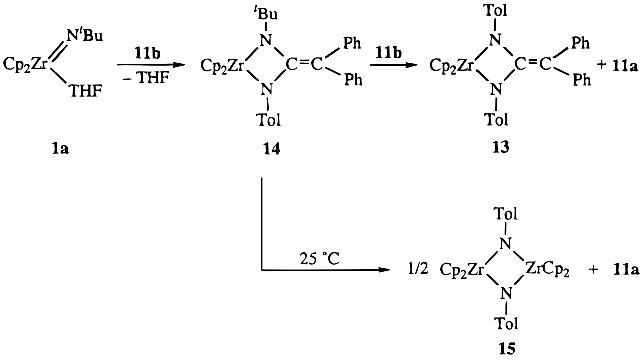

(**11b**) was prepared by literature methods.[50,51] The reaction of **1a** with 2 equiv of **11b** also spontaneously occurs at 25 °C to generate azametallacyclobutane $Cp_2Zr(NTol)_2C{=}CPh_2$ (**13**) and **11a** (Scheme 2). The ketenimine adduct **13** is cleanly generated at room temperature in toluene and can be isolated as black block crystals in 65% yield by recrystallization from toluene/pentane at −35 °C. Spectral data for **13** in C_6D_6 include new resonances for the *p*-tolyl methyl group at 2.08 ppm (6H) in the ^1H NMR and 20.9 ppm (CH_3) in the $^{13}C\{^1H\}$ NMR.

Monitoring this reaction by ^1H NMR spectrometry revealed a stepwise process that is dependent upon the concentration of **11b**. When a stoichiometric amount of **11b** is carefully introduced into a solution of **1a** at room temperature, azametallacyclobutane complex Cp_2Zr(N-*t*-Bu)(NTol)$C{=}CPh_2$ (**14**) is generated spontaneously as a major product (*ca.* 80% by ^1H NMR; 67% isolated) although some **13** is also generated (Scheme 2). That **14** is a 1:1 adduct of [$Cp_2Zr{=}$N-*t*-Bu] and **11b** is demonstrated by its ^1H NMR (C_6D_6) spectrum, which shows resonances due to the *tert*-butyl group at 0.93 ppm (9H) as well as a *p*-tolyl methyl resonance at 2.04 ppm (3H). When a second equivalent of **11b** is introduced, the product **14** instantly reacts to produce **13** and **11a**. In the absence of **11b**, at ambient temperature **14** is slowly converted to 0.5 equiv of the bridging imido dimer $(Cp_2ZrNTol)_2$ (**15**) and **11a**; **15** gradually precipitates from the solution. The latter reaction was driven to completion by heating to 45 °C and thin green needles of **15** were isolated in 42% isolated yield. An analogue of the bridging dimer **15**, $(Cp_2ZrNC_6H_4X)_2$ (X = H or CMe_3), has been synthesized previously by 1,2-elimination of $Cp_2Zr(NHC_6H_4X)(Me)$ at 85 °C.[10,11] It was also observed earlier in a zirconium-mediated imine metathesis reaction.[52,53]

Discussion

Mechanism of Imido/Oxo Exchange. The observations reported here and in earlier papers[10,39] suggest strongly that the reaction between imido complex **1a** and a wide range of carbonyl functionalities involves initial dissociation of THF, followed by overall [2 + 2] cycloaddition between the CO and the Zr=N moiety of the coordinatively unsaturated intermediate [$Cp_2Zr{=}$N-*t*-Bu],[10,11] to give oxaazametallacyclobutanes **6**. Similar [2 + 2] cycloadditions were observed in the reactions of **1a** with alkenes,[10] alkynes,[54] and imines,[52,53] where four-membered azametallacycles were isolated as products. In contrast, metallaoxetanes **6** cannot be isolated, although two such intermediates (**6b** and **6d**) were detected by low-temperature ^1H NMR spectrometry. The three types of carbonyl compounds that undergo this reaction, and the products they lead to, are summarized in Table 6.

Scheme 3

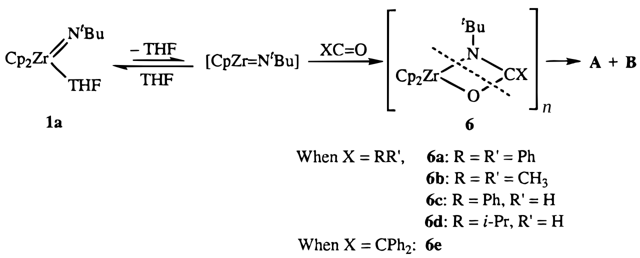

Table 6. Products Formed on Reaction of **1** with Three Different Classes of Carbonyl Compounds

XC=O	oxygen containing zirconocene products (**A**)	XC=N-*t*-Bu (**B**)
RR′C=O (**2b-d**)	$(Cp_2Zr{=}O)_n$ (**3**)	RR′C=N-*t*-Bu (**4b-d**)
$CpCo(CO)_2$ (**7**)	$(Cp_2Zr)_2(\mu\text{-}O)(\mu\text{-}N\text{-}t\text{-}Bu)$ (**9**)	CpCo(CO)(C=N-*t*-Bu) (**8a**)
$Ph_2C{=}C{=}O$ (**10**)	$(Cp_2Zr)_2O_3CCPh_2$ (**12**)	$Ph_2C{=}C{=}N$-*t*Bu (**11a**)

Scheme 4

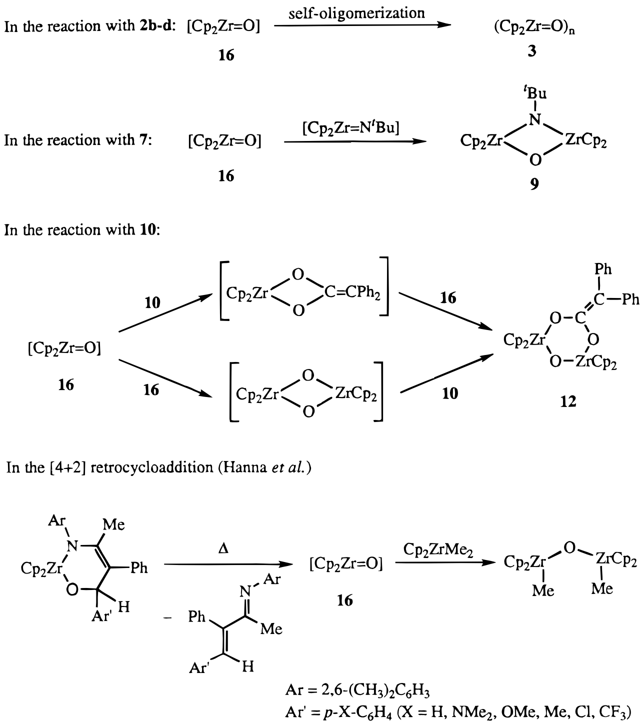

At first, we assumed that the reaction of an oxametallacyclobutane such as **6** would follow the known “Wittig-like” [2+2] ligand exchange process,[1,55−57] in which cycloreversion of **6** in the opposite sense would occur to provide the corresponding C=N bonded products and the transient $Cp_2Zr{=}O$ (**16**) which would rapidly oligomerize under the reaction conditions. However, the reactions of **1a** with various carbonyl sources revealed an interesting result: the nature of the oxo-containing zirconocene products (**A**, Table 6) depends upon the character of the carbonyl reagents. This situation is summarized in Scheme 4. For example, in contrast to the white precipitate of oligomeric $(Cp_2Zr{=}O)_n$ (**3**) that is produced when the imido complex **1a** is treated with organic carbonyls **2b−d**, only (μ-oxo)(μ-imido)dimer (**9**) is generated in the reaction of **1a** with metal carbonyls even under relatively vigorous reaction condi-

---

[50] Stevens, C. L.; French, J. C. *J. Am. Chem. Soc.* **1953**, *75*, 657.
[51] Stevens, C. L.; Singhal, G. H. *J. Org. Chem.* **1964**, *29*, 34.
[52] Meyer, K. E.; Walsh, P. J.; Bergman, R. G. *J. Am. Chem. Soc.* **1994**, *116*, 2669.
[53] Meyer, K. E.; Walsh, P. J.; Bergman, R. G. *J. Am. Chem. Soc.* **1995**, *117*, 974.
[54] Lee, S. Y.; Bergman, R. G. *Tetrahedron* **1995**, *51*, 4255.
[55] Cotton, F. A.; Hall, W. T. *J. Am. Chem. Soc.* **1979**, *101*, 5094.
[56] Rocklage, S. M.; Schrock, R. R. *J. Am. Chem. Soc.* **1980**, *102*, 7808.
[57] Nugent, W. A.; Harlow, R. L. *J. Chem. Soc., Chem. Commun.* **1978**, 579.

tions (2−3 days at 75 °C in THF). On the other hand, the reaction of **1a** with diphenylketene **10** produces neither oxozirconocene oligomer **3** nor (μ-oxo)(μ-imido)dimer **9** even in the presence of excess **1a**. Instead, it generates the tris-oxo complex **12** formed from two molecules of $Cp_2Zr{=}O$ (**16**) and one molecule of **10**. Furthermore, the formation of each product (**3**, **9**, or **12**) is not affected by modification of the reaction conditions such as changing the solvent or the ratio of the two starting materials. Finally, we[58] found recently that thermolysis of the 6-membered ring complex $Cp_2\overline{Zr{-}NArCMe{=}CPhCHAr'O}$ at 75 °C extrudes an α,β-unsaturated imine and provides yet another apparent source of $Cp_2Zr{=}O$. In this case in the absence of traps the oxo complex oligomerizes, as it does in the **1a** + **2b**−**d** reaction. However, when the thermolysis is run in the presence of Cp_2ZrMe_2, oligomerization is prevented and the apparent oxozirconocene intermediate is trapped quantitatively as the soluble μ-oxo complex $(Cp_2ZrMe)_2O$ (Scheme 4). Control experiments established that $[Cp_2Zr{=}O]_n$ (**3**) does not react with Cp_2ZrMe_2, even at 75 °C.

The divergent behavior of the postulated "$Cp_2Zr{=}O$" in these different reactions leads to the inescapable conclusion that the simple monomeric oxozirconocene complex cannot be the actual product-forming intermediate in every case. One might assume, for example, that transient **16** oligomerizes in the absence of any compound capable of trapping it, but in the presence of another molecule of [$Cp_2Zr{=}N$-*t*-Bu] it affords (μ-oxo)(μ-imido)dimer **9**. One must then ask why in the diphenylketene reaction no **9** is formed along with **12**, which requires two $Cp_2Zr{=}O$ fragments to ultimately find each other. Even more convincingly, addition of Cp_2ZrMe_2 to the reaction of **1a** with **2b**−**d** (or with **10**) still gives oligomer **3** (or tris-oxo complex **12**).[59] No diversion of the intermediate to $(Cp_2ZrMe)_2O$ is observed, in striking contrast to the observation made in the thermolysis of $Cp_2\overline{Zr{-}NArMe{=}CPhCHAr'O}$ described above.

To account for the behavior of **1a** with metal carbonyls, where (μ-oxo)(μ-imido) dimer **9** is formed, we suggest that stabilization of the $Cp_2Zr{=}O$ fragment **16** by coordination to another metal center may be occurring. Precedent for this can be found in Proulx and Bergman's report of the "Wittig type" metathesis of $CpTa({=}CH_2)(CH_3)$ with $PhRe(CO)_5$. Here an initial overall [2 + 2] addition, similar to the reaction between $Cp_2Zr{=}NR$ and $CpCo(CO)_2$, occurs that leads to a product in which $Cp_2(CH_3)Ta{=}O$ is weakly coordinated to a rhenium center.[60] In addition, a few other complexes in which a metal oxo moiety is coordinated to another metal center have been documented.[61,62] The similarity of these reactions suggests the possibility that the weak coordination of transient **16** to a metal carbonyl fragment (for example, as in **17**; Scheme 5) might prevent the self-oligomerization of the highly reactive $Cp_2Zr{=}O$ species, allowing it to react instead with [$Cp_2Zr{=}N$-*t*-Bu] to give (μ-oxo)(μ-imido)dimer **9** (path A in Scheme 5). Another possible way that the $Cp_2Zr{=}O$ fragment can remain attached to the cobalt carbonyl moiety is illustrated in path B in Scheme 5. Here only one Zr−N bond is initially cleaved in the first intermediate **18**, giving zwitterion **19**, which could rearrange as shown in the Scheme to give **9** and the isonitrile product.

Scheme 5

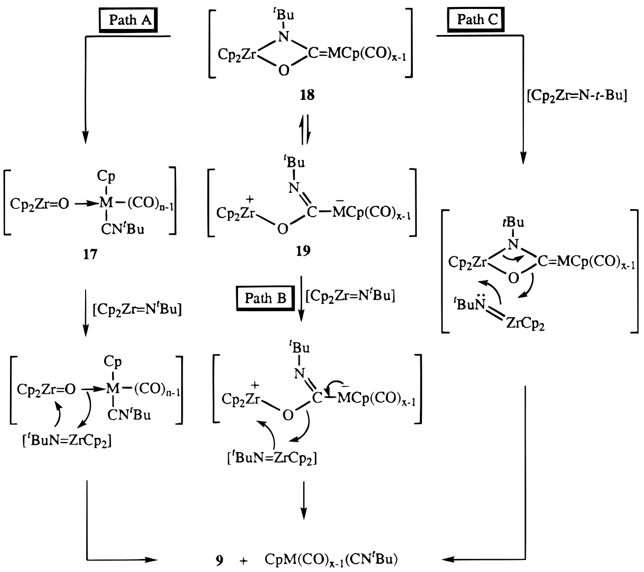

A third possible route to **9** that avoids free $Cp_2Zr{=}O$ is shown in path C of Scheme 5. Here intermediate **18** reacts directly with the transient imido complex $Cp_2Zr{=}N$-*t*-Bu to generate **9** in a concerted process. However, we do not see why such a mechanism should occur with the intermediate formed from metal carbonyl complexes but not with the analogous species that are presumably formed from ketones and ketenes.

Most perplexing is the reaction with diphenylketene, where two $Cp_2Zr{=}O$ fragments wind up in the final product, avoiding oligomerization or trapping with **1a**. Here we suggest that a dimeric intermediate formed early in the reaction might be involved.[63−71] An attractive possibility for this dimer is complex **20** in Scheme 6, since this only has to extrude 2 mol of the observed ketenimine product $Ph_2C{=}C{=}N$-*t*-Bu to generate the subsequent bis-μ-oxo intermediate $[Cp_2ZrO]_2$. Insertion of the C=O linkage of diphenylketene into a Zr−O bond in this intermediate leads to the observed product. The type of double coordination of oxygen to zirconium proposed for intermediate **20** is known, but it is influenced by the ring size of the oxametallacycle formed. For instance, oxametallacycloheptene complexes of zirconocene are mononuclear in solution and in the solid state[72] whereas smaller ring sizes (3-,[64,71] 4-,[63,70] and 5[65−69]-membered) of oxametallacycle derivatives are isolated as dimers. It therefore seems reasonable that the dimeric structure illustrated in Scheme 6 might be accessible to the

---

(58) Hanna, T. A.; Baranger, A. M.; Walsh, P. J.; Bergman, R. G. *J. Am. Chem. Soc.* **1995**, *117*, 3292.

(59) Under the reaction conditions (75 °C), **1a** reacts with Cp_2ZrMe_2 to give a mixture of products.

(60) Proulx, G.; Bergman, R. G. *J. Am. Chem. Soc.* **1993**, *115*, 9802.

(61) Housmekerides, C. E.; Ramage, D. L.; Kretz, C. M.; Shontz, J. T.; Pilato, R. S.; Geoffroy, G. L.; Rheingold, A. L.; Haggerty, B. S. *Inorg. Chem.* **1992**, *31*, 4453.

(62) Pilato, R. S.; Rubin, D.; Geoffroy, G. L.; Rheingold, A. L. *Inorg. Chem.* **1990**, *29*, 1986.

(63) Vaughan, G. A.; Hillhouse, G. L.; Lum, R. T.; Buchwald, S. L.; Rheingold, A. L. *J. Am. Chem. Soc.* **1988**, *110*, 7215.

(64) Erker, G.; Hoffmann, U.; Zwettler, R.; Betz, P.; Krüger, C. *Angew. Chem., Int. Ed. Engl.* **1989**, *28*, 630.

(65) Takaya, H.; Yamakawa, M.; Mashima, K. *J. Chem. Soc., Chem. Commun.* **1983**, 1283.

(66) Erker, G.; Dehnicke, S.; Rump, M.; Krüger, C.; Werner, S.; Nolte, M. *Angew. Chem., Int. Ed. Engl.* **1991**, *30*, 1349.

(67) Erker, G.; Mena, M.; Krüger, C.; Noe, R. *J. Organomet. Chem.* **1991**, *402*, 67.

(68) Erker, G.; Hoffmann, U.; Zwettler, R. *J. Organomet. Chem.* **1989**, *367*, C15.

(69) Mashima, K.; Yamakawa, M.; Takaya, H. *J. Chem. Soc., Dalton Trans.* **1991**, 2851.

(70) Erker, G.; Mena, M.; Krüger, C.; Noe, R. *Organometallics* **1991**, *10*, 1201.

(71) Bristow, G. S.; Hitchcock, P. B.; Lappert, M. F. *J. Chem. Soc., Chem. Commun.* **1982**, 462.

(72) Erker, G.; Engel, K.; Atwood, J. L.; Hunter, W. E. *Angew. Chem., Int. Ed. Engl.* **1983**, *22*, 494.

Scheme 6

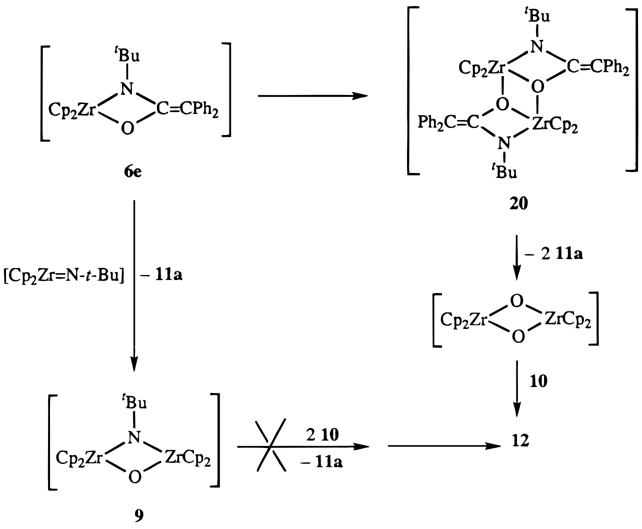

4-membered oxametallacycle **6e**. We considered the possibility that (μ-oxo)(μ-imido)dimer **9** might form in the reaction of **1a** with diphenylketene, and could then undergo further reaction with **10** to form the tris-oxo product **12**. However, a control experiment showed that **9** does not react with diphenylketene under the **1a** + diphenylketene reaction conditions.

Note Added in Proof. If dimer **20** and μ-oxo dimer $[Cp_2Zr{=}O]_2$ are the reactive intermediates in the ketene reaction, it occurred to us that a dimer analogous to **20** might also be involved in the reaction of **1** with simple ketones. This could be the true identity of the metastable species **6b** (or **6d**) detected by NMR spectrometry when **1** is allowed to react with ketones **2b** (or **2d**) at low temperature (i.e., $n = 2$ in the structure of **6b** and **6d** shown earlier in this paper). As we have postulated with **20**, **6b** and **6d** ($n = 2$) should also be capable of decomposing to give $[Cp_2Zr{=}O]_2$ before $[Cp_2Zr{=}O]_n$ is formed. If this is the case, the μ-oxo dimer should be trappable by diphenylketene in the acetone reaction. To test this idea, we repeated the reaction of **1a** with acetone at −35 °C and again observed the formation of the intermediate **6b**. Rather than allowing this solution to warm and release imine **4b** and $[Cp_2Zr{=}O]_n$, diphenylketene was added. Workup of the reaction mixture gave imine but no $[Cp_2Zr{=}O]_n$; instead, as predicted, a quantitative yield of **12** was formed.

In summary, it seems likely that none of the reactions reported here extrude free $Cp_2Zr{=}O$. We think the most likely source of this intermediate is in the thermal fragmentation of $Cp_2\overline{Zr{-}NArCMe{=}CPhCHAr'O}$, since this is the one reaction in which we have been able to trap it with added Cp_2ZrMe_2, and the rate of this process exhibits a zeroth-order dependence on the concentration of the dimethylzirconium compound.

Mechanism of the Ketenimine Reaction. To determine whether the initial steps in the reaction of imido complex **1a** with diphenylketene seemed reasonable, we sought an analogous reaction with ketenimines that might proceed somewhat less rapidly and thereby allow us to detect reaction intermediates. We knew from the reaction of **1a** with diphenylketene that the ketenimine product $Ph_2C{=}C{=}N$-t-Bu (**11a**) is stable to further reaction with **1a**. We therefore investigated the reaction of **1a** with the less hindered ketenimine $Ph_2C{=}C{=}NTol$ (**11b**). As summarized in Scheme 2, here it was possible to establish that the reaction proceeded by initial overall [2 + 2] cycloaddition, because the azametallacycle **14** could be detected and characterized by spectroscopic methods. The product **14** was also observed to undergo overall [2 + 2] ring cleavage in the opposite direction, generating the N-*tert*-butyl ketenimine **11a** and dimer **15**. The driving force for these reactions must be the release of steric congestion caused by the presence of the N-*tert*-butyl group in **14**. Similar conversions were observed earlier in the zirconium-mediated imine metathesis reactions studied by Meyer and Bergman,[52,53] where azametallacyclobutane **19**, in the absence of excess imine, undergoes the elimination of imine to give dimeric $[Cp_2Zr(NPh)]_2$ (Scheme 7). Extrapolation of Meyer and Bergman's kinetic results suggests that the reaction of imido complex **1a** with ketenimine **11b** proceeds by a dissociative mechanism involving formation of the transient imido complex [$Cp_2Zr{=}NTol$], which either dimerizes to give **15** or can be trapped by more *N*-phenyl ketenimine **11a** to give isolable adduct **13** as shown in Scheme 8.

Scheme 7

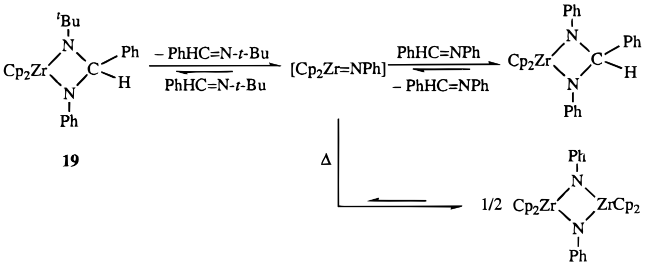

Scheme 8

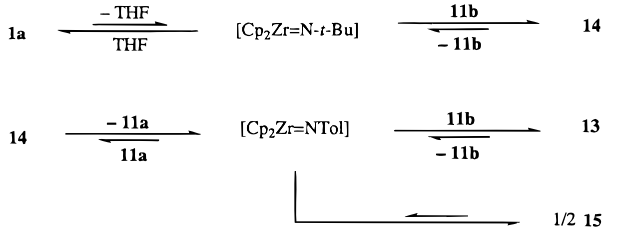

Summary

Imido/oxo exchange reactions between $Cp_2Zr{=}N$-t-Bu (**1a**) and various organic and organometallic carbonyl compounds have been investigated. The reactivity of **1a** toward organic carbonyl compounds (aldehydes and ketones) depends strongly on steric encumbrance and on the availability of α-hydrogens. Reactions with moderately hindered organic carbonyls **2e**−**g** generate the enolate complexes **5e**−**g**. In contrast, reactions with less hindered ketones and aldehydes **2b**−**d** undergo "Wittig-like" [2 + 2] cycloaddition/cycloreversion to form oxozirconocene oligomer **3** and imines **4b**−**d**. The reactions of **1a** with $CpCo(CO)_2$ (**7**) and $Ph_2C{=}C{=}O$ (**10**) also undergo imido/oxo exchange but lead to the new types of oxozirconocene-containing products (μ-oxo)(μ-imido) dimer **9** and tris-oxo complex **12**, respectively, instead of **3**. All these reactions ultimately extrude the $Cp_2Zr{=}O$ fragment, but because this moiety behaves differently in each reaction we do not believe it is generated as the free monomeric species in each transformation. In the reaction with metal carbonyls the fragment appears to be stabilized by coordination to the second "late" transition metal center, and we propose that the reaction with diphenylketene proceeds via a bis-μ-oxo zirconium dimer. It seems likely that $Cp_2Zr{=}O$ is generated as a free intermediate in the earlier-reported thermolytic fragmentation of Cp_2Zr(NArCMeCPhCRCHO), since it can be trapped by an external reagent in this reaction. Future work will be required to confirm these hypotheses and find ways to reliably generate and explore the chemistry of the elusive $Cp_2Zr{=}O$.

Experimental Section

General. For a description of the instrumentation and general procedures used, see earlier papers from this laboratory.[73]

Unless otherwise specified, all reagents were purchased from commercial suppliers and dried over activated molecular sieves (4 Å) before use. Volatile compounds were flash distilled under reduced pressure after drying (e.g. acetone (**2b**) and 2-methylpropanal (**2d**) were dried over activated molecular sieves and flash-distilled at reduced pressure). The metal carbonyl complexes $(C_6H_6)Cr(CO)_3$, $CpV(CO)_4$, and $CpRe(CO)_3$ were dissolved in benzene and dried over activated molecular sieves; the benzene was removed under reduced pressure after filtration. $CpCo(CO)_2$ was passed through a small column of activated alumina and distilled under reduced pressure. $CpMn(CO)_3$ was sublimed before use (40 °C, 100 mtorr). $CpFe(CH_3)(CO)_2$,[74,75] $Ph_2C{=}C{=}O$ (**10**),[49] and $Ph_2C{=}C{=}NTol$ (**11b**)[50,51] were prepared by the literature methods. Synthesis of compounds $Cp_2Zr({=}NR)(THF)$ ($R = C(CH_3)_3$ (**1a**), 2,6-$(CH_3)_2C_6H_4$ (**1b**)) are reported elsewhere.[10,11]

$(CH_3)_2C{=}N$-*t*-Bu (4b). To **1a** (69.7 mg, 0.19 mmol) in THF (1 mL) was added acetone (**2b**) (14 μL, 0.19 mmol). Upon addition of **2b**, the color of the solution temporarily changed from yellow to red-orange and a white solid precipitated from solution. The volatile materials (including THF) were collected by flash-distillation under reduced pressure and identified by GCMS and IR spectroscopy. The sample of **4b** for the ^{1}H and ^{13}C NMR data was separately prepared in THF-d_8 by the same procedure. ^{1}H NMR (400 MHz, THF-d_8): δ 1.88 (s, 3H, CH_3), 1.84 (s, 3H, CH_3), 1.20 (s, 9H, C(CH_3)$_3$). ^{13}C{^{1}H} NMR (400 MHz, THF-d_8): δ(C) 162.4, 54.9; δ(CH$_3$) 31.3, 30.8, 21.5. IR (THF): 1669 (s), 1457 (w), 1393 (w), 1356 (w) cm^{-1}.

Reactions of 1a with Organic Carbonyls 2c−d. An NMR tube was charged with **1a** (5 mg, 1.4×10^{-2} mmol) and excess **2c−d** (2−3 equiv) in THF-d_8 (0.4 mL). A white precipitate was produced upon mixing the reagents. A ^{1}H NMR spectrum of the reaction mixture showed resonances due to a new imine and several peaks around 6 ppm due to generation of $(Cp_2Zr{=}O)_n$ (**3**). The imine products **4c** and **4d** were identified by comparison of their spectra with literature spectral data. Compound **4c** was also confirmed by independent preparation. ^{1}H NMR (400 MHz, THF-d_8) of PhCH=N-*t*-Bu (**4c**): δ 8.27 (s, 1H, NH), 7.75 (d, J = 3.56 Hz, 2H, phenyl), 7.35 (m, 3H, phenyl), 1.26 (s, 9H, C(CH_3)$_3$) (lit.[21] ^{1}H NMR (CDCl$_3$): δ 8.32 (s, 1H, CH), 7.78−7.84 (m, 2H, phenyl), 7.40−7.45 (m, 3H, phenyl), 1.36 (s, 9H, C(CH_3)$_3$)). ^{1}H NMR (300 MHz, THF-d_8) of $(CH_3)_2CHCH{=}N$-*t*-Bu (**4d**): δ 7.52 (d, J = 4.17 Hz, 1H, CH), 2.30 (m, 1H, CH(CH$_3$)$_2$), 1.10 (s, 9H, C(CH_3)$_3$), 1.01 (d, J = 6.88 Hz, 6H, CH(CH_3)$_2$) (lit.[21,22] ^{1}H NMR (CDCl$_3$): δ 7.41 (d, J = 6.8 Hz, 1H, CH), 2.41 (m, 1H, CH(CH$_3$)$_2$), 1.16 (s, 9H, C(CH_3)$_3$), 1.05 (d, J = 5.9 Hz, 6H, CH(CH_3)$_2$)).

Spectroscopic Observation of $[Cp_2\overline{ZrOC(CH_3)_2N}$-*t*-Bu$]_2$ (6b). In the dry box, an NMR tube was charged with **1a** (26.4 mg, 7.2×10^{-2} mmol) in THF-d_8 (0.4 mL) and sealed with a rubber septum. The tube was removed from the drybox and cooled to −78 °C, then acetone (**2b**) (5.5 μL, 7.5×10^{-2} mmol) was injected by syringe. The tube was then shaken and inserted into a pre-cooled NMR probe (−50 °C): at this point ^{1}H NMR analysis showed an approximately 2:1 ratio of **6b** and **4b**. Conversion of the remaining **6b** to **4b** was monitored at −10 °C. At this temperature, resonances for products **4b** and **3** continued to grow as resonances for intermediate **6b** decreased in intensity. Upon warming to room temperature, the only major resonances observed were attributable to products **4b** and **3**. ^{1}H NMR (400 MHz, THF-d_8, −10 °C) of **6b**: δ 6.28 (s, 10H, C$_5H_5$), 1.34 (s, 6H, (CH_3)$_2$), 1.22 (s, 9H, C(CH_3)$_3$).

Low-Temperature NMR Study of the Reaction of 1a with $(CH_3)_2CHCHO$ (2d). In the drybox, an NMR tube was charged with $Cp_2Zr({=}N$-*t*-Bu)(THF) (**1a**) (20.1 mg, 5.5×10^{-2} mmol) in THF-d_8 (0.4 mL) and sealed with a rubber septum. The tube was removed from the box and cooled to −78 °C, then **2d** (4 mg, 5.6×10^{-2} mmol) was injected by syringe. At this point the tube was treated similarly to the reaction described above that was performed to observe **6b**. The tube was inserted into a pre-cooled probe set at −45 °C. The ^{1}H NMR spectrum of the reaction mixture showed an approximately 2:1:2:2 ratio of **4d**, **1a**, intermediate $[Cp_2\overline{ZrOCH(CH(CH_3)_2)N}$-*t*-Bu$]_2$ (**6d**), and another unidentified intermediate (resonances at δ 6.28, 4.42 (d), 1.68 (m), and 0.89). Upon increasing the temperature of the probe, resonances due to both intermediates decreased in intensity above −30 °C. The second intermediate disappeared faster than **6d** and conversion of **6d** to **4d** was only observed above 0 °C. ^{1}H NMR (400 MHz, THF-d_8, −10 °C) of **6d**: 6.96 ppm (d, J = 9.28 Hz, 1H, CH), 6.30 ppm (s, 10H, C$_5H_5$), 2.88 ppm (m, 1H, CH(CH$_3$)$_2$), 1.22 ppm (s, 9H, C(CH_3)$_3$), and 0.96 ppm (d, J = 9.30 Hz, 6H, CH(CH_3)$_2$).

$Cp_2Zr(NH$-*t*-Bu$)(O\overline{CCH(CH_2)_3C}HC(CH_3)_3)$ (5e). To a solution of 2-*tert*-butylhexan-1-one (**2e**) (102 mg, 0.66 mmol) in pentane was slowly added **1a** (220 mg, 0.60 mmol). The mixture was stirred for 1 h until the solution became homogeneous. Any pentane-insoluble material was removed by filtration and then the solvent and excess **2e** were removed under vacuum. The residual white solid was recrystallized from pentane at −35 °C to afford colorless crystals of **5e** (210 mg, 0.47 mmol, 78%). ^{1}H NMR (400 MHz, C$_6$D$_6$): δ 6.01 (s, 5H, C$_5H_5$), 5.95 (s, 5H, C$_5H_5$), 4.65 (br, 1H, NH), 4.52 (t, J = 4.08 Hz, 1H, CH(CH$_2$)$_3$), 2.23 (m, 2H, CH_2), 1.91 (m, 1H, CH(CH$_3$)$_3$), 1.74 (m, 2H, CH_2), 1.50 (m, 2H, CH_2), 1.23 (s, 9H, C(CH_3)$_3$), 1.13 (s, 9H, C(CH_3)$_3$). ^{13}C{^{1}H} NMR (400 MHz, C$_6$D$_6$): δ(C) 163.8, 56.6, 34.0; δ(CH) 110.8, 110.6, 101.7, 48.9; δ(CH$_2$) 27.6, 25.4, 23.1; δ(CH$_3$) 34.6, 30.1. IR (C$_6$D$_6$): 3340 (w), 2943 (s), 1633, 1475, 1374, 1273, 1217 (s), 1033, 977, 783, 691 cm^{-1}. Anal. Calcd for $C_{24}H_{37}NOZr$: C, 64.52; H, 8.35; N, 3.14. Found: C, 64.22; H, 8.33; N, 2.90.

Crystal Structure Determination of 5e. Colorless crystals of **5e** were obtained by two recrystallizations from pentane solution at −35 °C. A fragment having approximate dimensions of 0.20 × 0.25 × 0.30 mm was mounted on a glass fiber using Paratone N-hydrocarbon oil. All measurements were made on a Siemens SMART diffractometer with graphite monochromated Mo Kα radiation. Cell constants and an orientation matrix obtained from a least-squares refinement using the measured positions of 6597 reflections with $I > 3\sigma$ in the range $3.00 < 2\theta < 45.00°$ corresponded to a primitive monoclinic cell with the following dimensions: a = 9.4933(2) Å, b = 8.0068(2) Å, c = 30.6878(9) Å, β = 91.643(1)°, V = 2331.65(9) Å^3. For Z = 4 and fw = 445.77, the calculated density is 1.27 g/cm^3. The systematic absences of $h0l$: $h + l \neq 2n$ and $0k0$: $k \neq 2n$ uniquely determine the space group to be $P2_1/n$. The data were collected at a temperature of −103 ± 1 °C. Frame data were collected using ω scans of 0.3° and a total counting time of 10 s per frame.

Data were integrated using the program SAINT and box parameters of 1.6 × 1.6 x 0.6° out to a maximum 2θ value of 46.5°. The data were corrected for Lorentz and polarization effects. No decay correction was applied. The linear absorption coefficient μ for Mo Kα radiation is 4.8 cm^{-1}. The data were corrected for absorption using an empirical correction based on multiple measurements of equivalent reflections as calculated using the program XPREP (v. 5.03; part of the SHELXTL crystal structure determination program, Siemens Industrial Automation, Inc., Madison, WI (1995)) (μR = 0.06, T_{max} = 0.87, T_{min} = 0.81). The 9504 integrated and corrected reflections were averaged to yield 3600 unique reflections (R_{int} = 0.034).

The structure was solved by direct methods and expanded using Fourier techniques. Inspection of the model following refinement of most of the atoms with anisotropic thermal parameters showed a pattern of difference Fourier peaks consistent with a total disorder of the enolate ligand around a pseudo-mirror plane containing the O and C16 as shown in Figure 1. A major conformation contains C11−C20 and a minor one (see the supporting information) contains C211−C220. Peaks corresponding to all atoms of the disorder were located and refined with B_{iso} fixed to the average of the B_{iso} of the majority component. Adjustment of the disorder ratio revealed a shallow minimum in the residuals near an 18:82 ratio of two conformations. Hydrogen atoms were included in calculated positions for the majority component but not refined. The final cycle of full-matrix least-squares refinement was based on 2828 observed reflections ($I > 3.00\sigma(I)$) and 270 variable parameters and converged (largest parameter shift was 0.04 times its esd). The standard deviation of an observation of unit weight ($(\sum\omega(|F_o| - |F_c|)^2/(N_o - N_v))^{1/2}$: N_o = number of observations, N_v = number

---

[73] Baranger, A. M.; Bergman, R. G. *J. Am. Chem. Soc.* **1994**, *116*, 3822.

[74] Piper, T. S.; Wilkinson, G. *J. Inorg. Nucl. Chem.* **1956**, *3*, 104.

[75] Clifford, A. F.; Mukherjee, A. K. *J. Inorg. Nucl. Chem.* **1963**, *25*, 1065.

of variables) was 2.46. The weighting scheme was based on counting statistics and included a factor ($p = 0.031$) to downweight the intense reflections. The maximum and minimum peaks on the final difference Fourier map corresponded to 0.41 and -0.49 e$^-$/Å^3, respectively. The structure consists of separated molecules of the compound packed in the unit cell and there are no abnormally short intermolecular contacts.

$Cp_2Zr(NH$-*t*-Bu)OC(CH_2)-*t*-Bu (5f). To a solution of 3,3-dimethyl-2-butanone (**2f**) (52 mg, 0.52 mmol) in pentane was slowly added **1a** (150 mg, 0.41 mmol). The mixture was stirred for 1 h until the solution became homogeneous. Any pentane-insoluble material was removed by filtration and then the solvent and excess **2f** were removed under vacuum. The residual solid was recrystallized from pentane at -35 °C to provide colorless crystals of **5f** (134 mg, 0.34 mmol, 83%). ^{1}H NMR (400 MHz, C_6D_{12}): δ 6.09 (s, 10H, C_5H_5), 4.64 (br, 1H, NH), 3.78 (s, 1H, OCHH), 3.47 (s, 1H, OCHH), 1.18 (s, 9H, C(CH_3)$_3$), 1.02 (s, 9H, C(CH_3)$_3$). ^{13}C{^{1}H} NMR (400 MHz, C_6D_{12}): δ(C) 176.6, 56.8, 37.6; δ(CH) 111.3; δ(CH_2) 82.3; δ(CH_3) 34.9, 28.8. IR (C_6D_6): 3128, 2971 (s), 2907, 2879, 1595, 1365, 1300 (s), 1208 (s), 1189 (s), 1041, 986,792, 580 cm^{-1}. Anal. Calcd for $C_{20}H_{31}NOZr$: C, 61.17; H, 7.96; N, 3.57. Found: C, 61.10; H, 8.10; N, 3.33.

$Cp_2Zr(NH$-*t*-Bu)(OC(C(CH_3)$_2$)CH(CH_3)$_2$) (5g). A glass bomb (20 mL) was loaded with **1a** (119 mg, 0.33 mmol) and 2,4-dimethyl-3-pentanone (**2g**) (49 mg, 0.43 mmol) in THF (7 mL). The bomb was degassed with 1 freeze−pump−thaw cycle and heated to 45 °C for 5 h. After removal of solvent and excess ketone under reduced pressure, the residual white solid was recrystallized from pentane at -35 °C to provide white crystals of **5g** (102 mg, 0.25 mmol, 76%). ^{1}H NMR (400 MHz, C_6D_6): δ 5.96 (s, 10H, C_5H_5), 4.21 (br, 1H, NH), 2.88 (septet, $J = 6.85$ Hz, 1H, (CH_3)$_2$CH), 1.77 (s, 3H, CH_3), 1.76 (s, 3H, CH_3), 1.24 (s, 9H, C(CH_3)$_3$), 1.11 (d, $J = 6.85$ Hz, 6H, (CH_3)$_2$CH). ^{13}C{^{1}H} NMR (400 MHz, C_6D_6): δ(C) 159.8, 98.6, 56.5; δ(CH) 111.5, 30.4; δ(CH_3) 34.6, 20.6, 19.1, 18.8. IR (C_6D_6): 3350 (w), 3103 (w), 2961 (s), 2731 (w), 1660, 1475, 1387, 1360, 1271 (s), 1210 (s), 1077 (s), 1033, 989, 775 cm^{-1}. Anal. Calcd for $C_{21}H_{33}NOZr$: C, 62.02; H, 8.18; N, 3.44. Found: C, 61.90; H, 8.25; N, 3.31.

CpCo(CO)(CN-*t*-Bu) (8a). A glass bomb (50 mL) was loaded with **1a** (361 mg, 0.99 mmol) and CpCo(CO)$_2$ (**7**) (546 mg, 3.03 mmol) in THF (*ca.* 20 mL). The bomb was degassed with 1 freeze−pump−thaw cycle and heated to 75 °C for 1.5 days. After the solvent and excess **7** were removed under reduced pressure, the residual solid was extracted with pentane. The pentane solution was passed through a small column (0.25 in. by 2 in.) of activated alumina to remove residual (Cp_2Zr)$_2$(μ-O)(μ-N-*t*-Bu) (**9**). Evaporation of pentane from the filtrate afforded red solid **8a** (62 mg, 0.26 mmol, 53%). ^{1}H NMR (400 MHz, C_6D_6): δ 4.76 (s, 5H, C_5H_5), 0.90 (s, 9H, C(CH_3)$_3$). ^{13}C{^{1}H} NMR (400 MHz, C_6D_6): δ(C) 208.4, 161.6, 57.0; δ(CH) 82.7; δ(CH_3) 30.5. IR (Nujol): 2990, 2117, 2072, 2028, 1948, 1375, 1217 cm^{-1}. (lit.[41] ^{1}H NMR (C_6D_6): δ 4.75 (s, 5H, C_5H_5), 0.91 (s, 9H, C(CH_3)$_3$)).

CpCo(^{13}CO)$_2$ (7-^{13}C). A glass bomb (10 mL) was loaded with CpCo(CO)$_2$ (**7**) (170 mg, 0.47 mmol). After the bomb was degassed with 2 freeze−pump−thaw cycles, it was filled with ^{13}CO to 1.5 atm and shaken for 1 day. This process was repeated one more time. Two cycles of ^{13}CO exchange provided 86 ± 4% ^{13}CO labeled CpCo(^{13}CO)$_2$ (**7-^{13}C**). ^{13}C incorporation of **7-^{13}C** was determined by EI mass spectroscopy (determined by integration of relative mass peaks) as well as ^{13}C NMR spectra and IR spectra.

CpCo(^{13}CO)(^{13}CN-*t*-Bu) (8a-^{13}C). CpCo(^{13}CO)(^{13}CN-*t*-Bu) was prepared in a fashion analogous to the synthesis of **8a** except that 86% ^{13}CO labeled CpCo(^{13}CO)$_2$ (**7-^{13}C**) was used in place of unlabeled **7**. EI mass spectroscopy as well as spectral data (^{13}C NMR spectra and IR) showed that CpCo(^{13}CO)(^{13}CN-*t*-Bu) was generated with 84 ± 4% incorporation of ^{13}C label.

(Cp_2Zr)$_2$(μ-O)(μ-N-*t*-Bu) (9). A glass bomb (50 mL) was loaded with **1a** (361 mg, 0.99 mmol) and CpCo(CO)$_2$ (**7**) (546 mg, 3.03 mmol) in THF (*ca.* 20 mL). The reaction mixture was degassed with 1 freeze−pump−thaw cycle and heated to 75 °C for 1.5 days. After removal of solvent and excess **7** under reduced pressure, the residual solid was washed with pentane. The pentane-insoluble material was then collected and dissolved in warm Et_2O. Slow evaporation of Et_2O from the solution at room temperature afforded block red crystals of **9** (79 mg, 0.15 mmol, 30%). ^{1}H NMR (400 MHz, C_6D_6): δ 6.10 (S, 20H, C_5H_5), 1.12 (s, 9H, C(CH_3)$_3$). ^{13}C{^{1}H} NMR (400 MHz, C_6D_6): δ(C) 62.9; δ(CH) 112.1; δ(CH_3) 37.3. IR (C_6D_6): 2959, 2356, 1168, 1027, 791, 631 (s) cm^{-1}. MS (EI): *m/e* 529.9 (M$^+$). Anal. Calcd for $C_{24}H_{29}NOZr_2$: C, 54.40; H, 5.52; N, 2.64. Found: C, 54.65; H, 5.82; N, 2.52.

CpCo(CO)(2,6-(CH_3)$_2C_6H_3$NC) (8b). A glass bomb was charged with **1b** (208 mg, 0.57 mmol) and **7** (321 mg, 1.78 mmol) in C_6H_6 (10 mL). The bomb was degassed with 1 freeze−pump−thaw cycle, heated to 75 °C for 1 day, and then analyzed by ^{1}H NMR spectrometry. No major resonances near 6 ppm were observed, but resonances attributable to CpCo(CO)(2,6-(CH_3)$_2C_6H_3$NC) (**8b**) were generated during the reaction. After the zirconium-containing products were removed from the reaction mixure by filtration through florisil (×2), the red solution was chromatographed on silica gel (using a 1:1 ratio of hexane and benzene) to separate **8b** from CpCo(2,6-(CH_3)$_2C_6H_3$NC)$_2$[43] (12% by ^{1}H NMR) and to afford **8b** as a red-brown solid (72.6 mg, 0.26 mmol, 46%). ^{1}H NMR (400 MHz, C_6D_6) of CpCo(CO)$_2$(2,6-(CH_3)$_2C_6H_3$-NC): δ 6.72 (t, $J = 7.48$ Hz, 1H, aryl), 6.63 (d, $J = 7.41$ Hz, 2H, aryl), 4.79 (s, 5H, C_5H_5), 2.08 (s, 6H, CH_3). ^{13}C{^{1}H} NMR (400 MHz, C_6D_6): δ(C) 133.8, 130.2, 128.5; δ(CH) 127.8, 126.4, 83.3; δ(CH_3) 18.6 (one quaternary C was not located). IR (C_6D_6): 2071, 1955 cm^{-1} (lit.[43] IR (C_6D_6): 2075, 1956 cm^{-1}).

Reactions of 1a with Various Metal Carbonyls (CpV(CO)$_4$, CpFe(CH_3)(CO)$_2$, (C_6H_6)Cr(CO)$_3$, or Mo(CO)$_6$). An NMR tube was charged with **1a** (14 mg, 3.8×10^{-2} mmol) and a metal carbonyl complex (3 equiv) in THF-d_8 (0.5 mL). The tube was degassed with 1 freeze−pump−thaw cycle and sealed on a vacuum line. The reaction was then monitored using ^{1}H NMR until no starting imido complex **1a** was observed (2.5 days at 25 °C for CpV(CO)$_4$, 1 day at 75 °C for CpFe(CH_3)(CO)$_2$, 6 h at 25 °C for (C_6H_6)Cr(CO)$_3$, and 15 h at 25 °C for Mo(CO)$_6$). The reactions proceeded cleanly by ^{1}H NMR and always generated new resonances at 6.25 (20H) and 1.31 (9H) ppm due to formation of **9**. The corresponding isocyanide complex (CpV(CO)$_3$-(CN-*t*-Bu), CpFe(CH_3)(CO)(CN-*t*-Bu), or C_6H_6Cr(CO)$_2$(CN-*t*-Bu), respectively) was also generated except for the reaction of Mo(CO)$_6$ in which several *tert*-butyl resonances near 1.5 ppm were observed (presumably due to formation of a mixture of Mo(CO)$_{6-n}$(CN-*t*-Bu)$_n$). Zirconium-containing **9** was removed by passing the solution through a small column of activated alumina. Evaporation of the solvent from the filtrate afforded the isocyanide product and excess metal carbonyl complex. The ^{1}H NMR spectra of the isocyanide products were compared to literature spectral data. ^{1}H NMR (300 MHz, C_6D_6) of CpV(CO)$_3$(CN-*t*-Bu): δ 4.57 (s, 5H, C_5H_5), 0.89 (s, 9H, C(CH_3)$_3$) (lit.[44] ^{1}H NMR (C_6D_6): δ 4.58 (s, 5H, C_5H_5), 0.90 (s, 9H, C(CH_3)$_3$)). ^{1}H NMR (300 MHz, $CDCl_3$) of CpFe(CH_3)(CO)(CN-*t*-Bu): δ 4.48 (s, 5H, C_5H_5), 1.38 (s, 9H, C(CH_3)$_3$), -0.07 (s, 3H, CH_3) (lit.[45] ^{1}H NMR ($CDCl_3$): δ 4.62 (s, 5H, C_5H_5), 1.44 (s, 9H, C(CH_3)$_3$), -0.06 (s, 3H, CH_3)). ^{1}H NMR (400 MHz, $CDCl_3$) of (C_6H_6)Cr(CO)$_2$(CN-*t*-Bu): δ 4.93 (s, 6H, C_6H_6), 1.37 (s, 9H, C(CH_3)$_3$) (lit.[47] ^{1}H NMR ($CDCl_3$): δ 5.43 (s, 6H, C_6H_6), 1.38 (s, 9H, C(CH_3)$_3$)).

Reactions of 1a with CpM(CO)$_3$ (M = Mn, Re) in THF-d_8. An NMR tube was charged with **1a** (12 mg, *ca.* 33 μmol) and CpM(CO)$_3$ (M = Mn, Re) (3 equiv) in THF-d_8 (0.4 mL). The tube was degassed with 1 freeze−pump−thaw cycle and sealed on a vacuum line. The reaction mixture was heated to 110 (M = Re) or 135 °C (M = Mn) for 3.5 days and monitored by ^{1}H NMR spectrometry. The ratio of products was measured by one-pulse integration of the ^{1}H NMR spectra. In the reaction of CpMn(CO)$_3$, *ca.* 60% of Cp_2Zr(NH-*t*-Bu)(η^1:η^5-C_5H_4)Mn(CO)$_3$ was generated and *ca.* 30% of **9** observed. In the reaction of CpRe(CO)$_3$, *ca.* 85% of Cp_2Zr(NH-*t*-Bu)(η^1:η^5-C_5H_4)Re(CO)$_3$ and (Cp_2Zr)$_2$(NH-*t*-Bu)$_2$(η^1:η^1:η^5-C_5H_3)Re(CO)$_3$ were observed and only 15% of **9** was generated. During both reactions, *tert*-butyl resonances at 1.15 ppm were generated (presumably due to formation of CpM(CO)$_2$(CN-*t*-Bu) (M = Mn, Re)), but not clearly indentified due to the complex nature of the spectra. The spectral data for Cp_2Zr(NH-*t*-Bu)(η^1:η^5-C_5H_4)Mn(CO)$_3$, Cp_2Zr(NH-*t*-Bu)(η^1:η^5-C_5H_4)Re(CO)$_3$, and (Cp_2Zr)$_2$(NH-*t*-Bu)$_2$(η^1:η^1:η^5-C_5H_3)Re(CO)$_3$ are reported elsewhere.[39,40]

$Ph_2C{=}C{=}N$-*t*-Bu (11a). There are three ways to obtain ketenimine generated as a by-product during the synthesis of **12**, **13**, and **15**. Isolation of **11a** from those reactions is described below. (A) The procedure was the same as that used in the synthesis of **12**. After crystallization of **12**, the mother liquor was passed through dried florisil (5 × 0.8 cm) two times to destroy any residual zirconium-containing compounds. Evaporation of the filtrate under reduced pressure afforded **11a** as a yellow oil (43 mg, 0.17 mmol, 71%). (B) The procedure was the same as that used in the synthesis of **13**. After **13** was crystallized from the pentane solution, the mother liquor was passed through florisil (5 × 0.8 cm) two times to destroy any residual zirconium-containing compounds. Evaporation of the filtrate under reduced pressure also afforded **11a** as a yellow oil (62 mg, 0.25 mmol, 58%). (C) The reaction procedure was the same as that used in the synthesis of **15**. After isolation of insoluble **15**, the mother liquor was passed through florisil to destroy any residual zirconium-containing compounds. Removal of the solvent from the filtrate under reduced pressure also afforded **11a** (25 mg, 0.10 mmol, 73%). Several attempts failed to give material suitable for elemental analysis and so the ketenimine was characterized spectroscopically. ^{1}H NMR (400 MHz, C_6D_6): δ 7.41 (d, $J = 8.4$ Hz, 4H, Ar-*H*), 7.15 (dd, $J = 7.93$ Hz, $J = 7.6$ Hz, 4H, Ar-*H*), 7.15 (t, $J = 7.39$ Hz, 2H, Ar-*H*), 1.16 (s, $C(CH_3)_3$, 9H). ^{13}C-{^{1}H} NMR (400 MHz, C_6D_{12}): δ(C) 183.1, 136.4, 60.3; δ(CH) 129.0, 127.9, 126.0; $\delta(CH_3)$ 30.8 (one quaternary C was not located). IR (THF): 2015 (s), 1601, 1742, 1496, 757, 695 cm^{-1}.

$(Cp_2Zr)_2O_3CCPh_2$ (12). To a solution of **1a** (89 mg, 0.24 mmol) in 10 mL of C_6H_6 was added $Ph_2C=C=O$ (**10**) (111 mg, 0.57 mmol). Upon the addition of **10**, the color of the solution changed from yellow to orange. The solution was then stirred for 10 min. Slow vapor diffusion of pentane into the solution followed by slow cooling to −35 °C afforded orange crystals of **12** (53 mg, 7.9×10^{-2} mmol, 65%). ^{1}H NMR (400 MHz, THF-d_8): δ 7.34 (dd, $J = 8.2$ Hz, $J = 1.1$ Hz, 4H, Ph-*H*), 7.15 (dd, $J = 8.1$ Hz, $J = 7.5$ Hz, 4H, Ph-*H*), 6.91 (dd, $J = 7.3$ Hz, $J = 1.2$ Hz, 2H, Ph-*H*), 6.35 (s, 20H, C_5H_5). ^{13}C{^{1}H} NMR (400 MHz, THF-d_8): δ(C) 166.8, 144.7, 90.5; δ(CH) 130.8, 127.7, 123.0, 114.0. IR (THF): 3110 (w), 1536 (s), 1329 (w), 1319 (w), 1018 (w), 989 (w), 772, 697, 612, 556, 480 cm^{-1}. HRMS (EI) *m/e* calcd for $C_{34}H_{30}O_3Zr_2$ 668.0308 (M$^+$); found 668.0305 (M$^+$).

Crystal Structure Determination of [12·0.5THF]. A yellow crystal of **12** (which turned out to be the cyclic organometallic complex crystallized with 0.5 molecules of THF) was obtained by slow vapor diffusion of pentane into a THF solution followed by cooling to −35 °C. A fragment cleaved from this crystal was mounted as described for **5e**. X-ray data were collected as for **5e** except that an Enraf-Nonius CAD-4 diffractometer was used. The final cell parameters and specific data collection parameters for this data set are given in Table 1.

The 3022 raw intensity data were converted to structure factor amplitudes and their esd's by correction for scan speed, background, and Lorentz and polarization effects. No correction for crystal decomposition was necessary. An empirical absorption correction based on azimuthal scan data was applied to the data ($T_{max} = 0.998$, $T_{min} = 0.934$, used by the program DIFABS in MOLEN). The structure was solved by Patterson methods and refined *via* standard least-squares and Fourier techniques (hydrogen atoms ignored). The final residuals for 179 variables refined against the 1753 data set for which $F^2 > 3\sigma(F^2)$ are given in Table 1. The largest peak in the final difference Fourier map had an electron density of 0.66 e$^-$/A^3, and the lowest excursion was −0.27 e$^-$/A^3. The *p*-factor, used to reduce the weight of intense reflections, was set to 0.03 in the last cycles of refinement. Only the zirconium atom was refined with anisotropic thermal parameters.

$Cp_2Zr(NTol)_2C=CPh_2$ (13). To **1a** (156 mg, 0.43 mmol) in 20 mL of toluene was added $Ph_2C=C=NTol$ (**11b**) (244 mg, 0.86 mmol). Upon addition of **11b**, the color of the solution changed from yellow to dark brown. The solution was stirred for 1 h and the solvent was removed under reduced pressure. The residue was washed with pentane and recrystallized from toluene layered with pentane at −35 °C to afford dark brown block crystals of **13** (169 mg, 0.28 mmol, 65%). The pentane extract mostly consisted of $Ph_2C=C=N$-*t*-Bu (**11a**), but some **13** was also dissolved in the solution. Dark brown crystals of **13** would also be grown from the pentane solution at −35 °C. ^{1}H NMR (400 MHz, C_6D_6): δ 7.46 (dd, $J = 7.2$ Hz, $J = 1.1$ Hz, 4H, Ph-*H*), 7.09 (dd, $J = 7.4$ Hz, $J = 8.0$ Hz, 4H, Ph-*H*), 6.83 (d, $J = 8.1$ Hz, 4H, Tol-*H*), 6.80 (tt, $J = 7.4$ Hz, $J = 1.1$ Hz, 2H, Ph-*H*), 6.62 (d, $J = 8.1$ Hz, 4H, Tol-*H*), 5.88 (s, 10H, C_5H_5), 2.08 (s, 6H, CH_3). ^{13}C{^{1}H} NMR (400 MHz, C_6D_6): δ(C) 149.2, 144.8, 142.5, 129.3, 92.1; δ(CH) 130.8, 128.8, 127.7, 123.3, 120.1, 115.9; $\delta(CH_3)$ 20.9. IR (C_6D_6): 3075, 3039, 2958, 2913, 1965, 1505 (s), 1316, 810, 689 cm^{-1}. MS (EI): *m/e* 609.8 (M$^+$). Anal. Calcd for $C_{38}H_{34}N_2Zr$: C, 74.83; H, 5.62; N, 4.59. Found: C, 74.64; H, 5.74; N, 4.46.

Cp_2Zr(N-*t*-Bu)(NTol)$CCPh_2$ (14). To **1a** (156 mg, 0.43 mmol) in toluene (6 mL) was added $Ph_2C=C=NTol$ (**11b**) (122 mg, 0.43 mmol). Upon addition of **11b**, the color of the solution changed from yellow to dark brown. The solvent was immediately removed under reduced pressure. The residue was washed with pentane to remove $Ph_2C=C=N$-*t*-Bu (**11a**) and then recrystallized from toluene layered with pentane at −35 °C to afford **14** as a red-brown precipitate (165 mg, 0.29 mmol, 67%). Because **14** decomposes to **15** and **11a** at the ambient temperature, spectral data other than ^{1}H NMR were not obtained. ^{1}H NMR (400 MHz, C_6D_6): δ 7.38 (d, $J = 7.3$ Hz, 4H, Ph-*H*), 7.15 (t, $J = 7.6$ Hz, 4H, Ph-*H*), 6.89 (t, $J = 7.0$ Hz, 2H, Ph-*H*), 6.83 (d, $J = 8.2$ Hz, 2H, Tol-*H*), 6.76 (d, $J = 7.7$ Hz, 2H, Tol-*H*), 6.01 (s, 10H, C_5H_5), 2.04 (s, 3H, CH_3), 0.92 (s, 9H, $C(CH_3)_3$).

$[Cp_2Zr(NTol)]_2$ (15). A glass vessel with a vacuum stopcock (15 mL) was charged with **14** (79 mg, 0.14 mmol) in C_6H_6 (4 mL). The bomb was degassed with 1 freeze−pump−thaw cycle and heated to 45 °C for 1.5 days. A green solid precipitated from the solution; it was collected, rinsed 2 times with pentane, and recrystallized from THF layered with pentane at −35 °C to afford thin green needles of **15** (19 mg, 2.9×10^{-2} mmol, 42%). ^{1}H NMR (300 MHz, C_6D_6): δ 7.00 (d, $J = 7.9$ Hz, 4H, Tol-*H*), 6.25 (s, 20H, C_5H_5), 5.75 (d, $J = 8.3$ Hz, 4H, Tol-*H*), 2.35 (s, 6H, CH_3). ^{13}C{^{1}H} NMR (400 MHz, THF-d_8): δ(C) 156.1,126.1; δ(CH) 128.8, 121.0, 113.3; $\delta(CH_3)$ 20.6. IR (Nujol): 3076, 2510, 2368 (w), 2342 (w), 1705 (w), 1607, 1563, 1492 (s), 1245 (s), 1201, 1113, 1024, 891, 794 (s), 661, 573 cm^{-1}. MS (EI): *m/e* 650 (M$^+$). Anal. Calcd for $C_{34}H_{34}N_2Zr_2$: C, 62.53; H, 5.25; N, 4.29. Found: C, 62.48; H, 5.23; N, 4.44.

Acknowledgment. We acknowledge the National Institutes of Health (Grant No. R37-GM25459) for generous financial support of this work. We are grateful to Dr. F. J. Hollander, staff crystallographer of the U.C. Berkeley X-ray diffraction facility (CHEXRAY), for determination of the X-ray structures.

Supporting Information Available: Tables of X-ray diffraction data (positional and anisotropic thermal parameters and full intramolecular distances and angles) for **5e** and **12** (23 pages). Ordering information is given on any current masthead page.

JA954050T